

REVIEW SUMMARY

PLANT SCIENCE

The mechanics of plant morphogenesis

Enrico Coen* and Daniel J. Cosgrove*

BACKGROUND: The growth and shape of plants depend on the mechanical properties of the plant's mesh of interconnected cell walls. Because adhering cell walls prevent cell migrations, morphogenesis is simpler to study in plants than in animals. Spatiotemporal variations in the rates and orientations at which cell walls yield to mechanical stresses—ultimately powered by cell turgor pressure—underlie the development and diversity of plant forms. Here, we review new insights and points of current contention in our understanding of plant morphogenesis, starting from wall components and building up to cells and tissues.

ADVANCES: Recent modeling and experimental studies have enabled advances at four levels: fiber, wall, cell, and tissue. In moving up levels, a population of discrete components is typically abstracted to a continuum at the next level (e.g., fibers to wall, walls to cell, cells to tissue). These abstractions help to both clarify concepts and simplify simulations. Mechanical stresses operate at each level, but values are typically not the same from one level to the next.

At the fiber level, growth corresponds to cellulose microfibrils sliding past each other, which is passively driven by turgor-induced tension. The rate of sliding depends on adhesion between microfibrils, whereas anisotropy reflects differences in the proportion of fibers in different orientations. Growth occurs preferentially in the direction of maximal microfibril stress.

At the wall level, microfibril sliding corresponds to cell wall creep, at rates dependent on turgor, wall extensibility, thickness, and yield thresholds. Anisotropic mechanical properties can arise through orientation-selective synthesis of cellulose microfibrils, guided by microtubules. Creep is stimulated by the wall-

loosening action of expansins, which increase extensibility and lower the yield threshold. Wall synthesis and loosening influence growth in complementary ways. Wall loosening increases growth rate with almost immediate effect, but unless wall synthesis increases in parallel, wall thickness declines over time, potentially weakening the wall. Wall synthesis requires a longer time scale to have a discernible growth effect but is critical for maintaining wall thickness and orienting anisotropy. By regulating loosening and synthesis separately, plants have the flexibility to produce rapid growth responses as well as control longer-term growth patterns and mechanical strength.

At the cellular level, growth corresponds to irreversible deformations that are catalyzed by expansins and physically driven by mechanical stresses that arise from turgor acting on cell walls. Oriented cell growth depends on wall anisotropy and cell geometry, which in turn depend on the dynamics of microtubule alignment. Collisions between microtubules lead to self-organized alignments that may be influenced by cellular cues and cell geometry.

At the tissue level, cell-cell adhesion combined with differential wall properties can lead to tissue-wide stresses. Tissue morphogenesis depends on coupling the mechanical properties of walls, cells, and tissues to regional patterning. Coupling may occur by regional gene activity that modifies rates of microfibril deposition, wall extensibility, and/or yield thresholds, and thus wall growth through creep. Regional gene activity may also provide tissue cues that orient microtubule alignments, and thus the orientations of growth anisotropy. Computational modeling, informed by developmental genetics, live imaging, and growth analysis, has shown how these principles can

account for morphogenetic changes through mechanically connected tissue regions irreversibly growing at specified rates and orientations. Taken as a whole, the cellulose network at the fiber and wall level provides elastic resistance to deformation while allowing growth through creep, which enables morphogenesis at the cell and tissue level while maintaining mechanical strength.

OUTLOOK: A key question is how patterns of gene expression at the tissue level modify behaviors and mechanics at other levels to generate tissue morphogenesis. Although we outline broad principles for how this may operate, many of the underlying molecular mechanisms remain unresolved. Controversies remain over the role of pectins in controlling wall mechanics and in the role of mechanosensing, chemical signaling, and polarity in controlling orientations of growth. And although tissue-level models have been proposed to account for morphogenetic changes, many of the underlying components remain hypothetical. A further challenge is to determine how interactions across levels have been modified during evolution to give rise to the diversity of plant forms.

Many of the principles described here may also be applicable to microbial and animal morphogenesis. Similar to plants, rates and orientations of cellular growth in these organisms depend on fibers in the wall or cell cortex that resist turgor. Controlled fiber sliding may play a key role, though in animals such sliding can be driven actively as well as passively. In animal tissues where cell rearrangements are limited, as during organogenesis, growth coordination and tissue stresses may operate similarly to plants. Thus, although the molecular players that control plant, animal, and microbial development are different, the mechanics of morphogenesis may share common principles. ■

The list of author affiliations is available in the full article online.

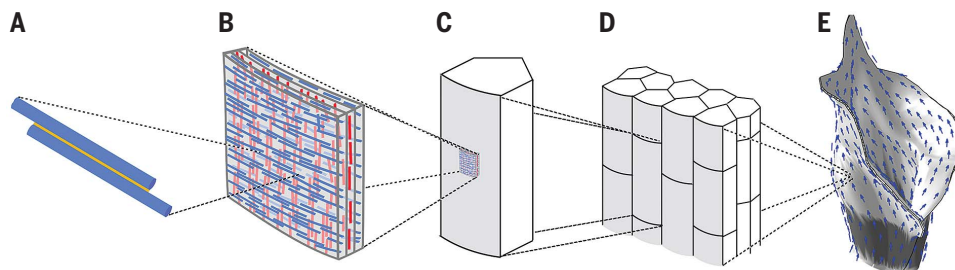
*Corresponding author. Email: enrico.coen@jic.ac.uk (E.C); dcosgrove@psu.edu (D.J.C.)

Cite this article as E. Coen and D. J. Cosgrove, *Science* 379, eade8055 (2023). DOI: 10.1126/science.ade8055

S READ THE FULL ARTICLE AT
<https://doi.org/10.1126/science.ade8055>

Plant morphogenesis, from nano- to

macroscale. (A to E) Growth begins with the sliding of cellulose fibers (A) within the cohesive, extensible, and layered networks of cell walls [(B); layers with different fiber orientations are color coded]. Sliding is physically driven by turgor pressure, which generates stress patterns in cells (C) and across tissues (D). Patterned tissue growth may be oriented by polarity fields (arrows) to generate complex forms (E).



REVIEW

PLANT SCIENCE

The mechanics of plant morphogenesis

Enrico Coen^{1*} and Daniel J. Cosgrove^{2*}

Understanding the mechanism by which patterned gene activity leads to mechanical deformation of cells and tissues to create complex forms is a major challenge for developmental biology. Plants offer advantages for addressing this problem because their cells do not migrate or rearrange during morphogenesis, which simplifies analysis. We synthesize results from experimental analysis and computational modeling to show how mechanical interactions between cellulose fibers translate through wall, cell, and tissue levels to generate complex plant tissue shapes. Genes can modify mechanical properties and stresses at each level, though the values and pattern of stresses differ from one level to the next. The dynamic cellulose network provides elastic resistance to deformation while allowing growth through fiber sliding, which enables morphogenesis while maintaining mechanical strength.

The growth and shape of plants depend on the mechanical properties of the plant's mesh of interconnected cell walls. Because adhering cell walls prevent cell migrations, morphogenesis is simpler to study in plants than in animals. Spatiotemporal variations in the rates and orientations at which cell walls yield to mechanical stresses—ultimately powered by cell turgor pressure—underlie the development and diversity of plant forms. Considerable progress has been made in understanding the molecular genetic basis of plant morphogenesis, but confusion and controversies remain over how these findings relate to the mechanics of development. Here, we review new insights and points of current contention in our understanding of the mechanics of plant morphogenesis, starting from wall components and building up to cells and tissues.

At the heart of morphogenesis is a trade-off between mechanical stiffness and deformability. As a plant develops, it must resist external mechanical forces, such as gravity and wind, while also growing by several orders of magnitude and deforming to produce its characteristic shapes. Plant materials therefore need to be strong while also pliant enough to grow and deform. These conflicting requirements are partly met by restricting morphogenesis to protected areas such as embryos, growing tips (apical meristems), and cambial zones, which reduces the extent to which they weaken the plant. However, even within these zones, mechanical strength needs to be maintained. A key problem is how such strength is achieved in the face of growth.

Fiber mechanics

The mechanical properties of plant tissues largely depend on how fibers in cell walls are organized. These fibers experience tensile stress caused by turgor pressure of several atmospheres within each cell, which provides the primary driving force for plant growth (1–3). Non-turgor-based mechanisms, in which growth is driven by active insertion of cell wall material, have been proposed (4, 5), but their contribution to plant growth remains contentious (1, 6).

The main load-bearing fibers are cellulose microfibrils, each comprising many linear β 1,4-glucan chains packed into a crystalline array, with stiffness comparable to steel. Aligned microfibrils bind strongly to each other laterally, forming two-dimensional networks that resist being stretched (7). Microfibrils are embedded in a hydrophilic matrix of pectins and hemicelluloses that make up

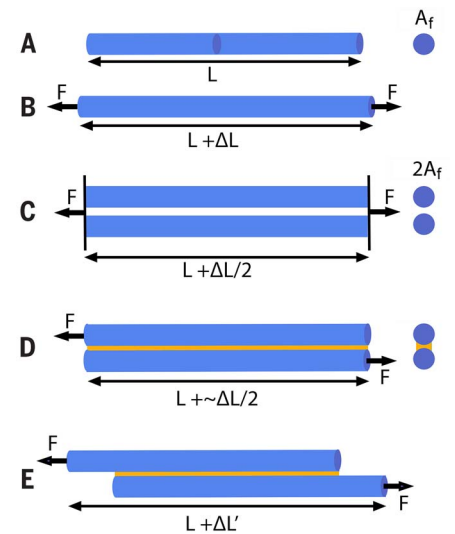
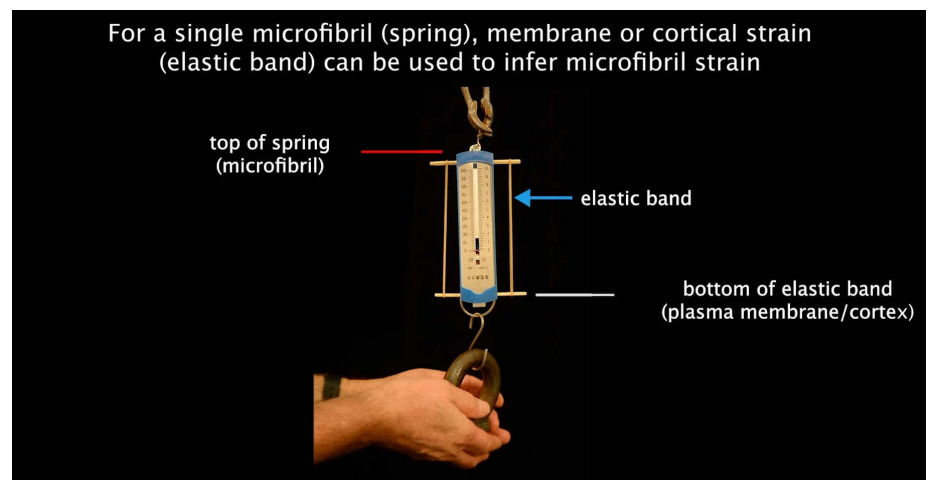


Fig. 1. Fiber growth in one dimension. (A) Fiber of length L and cross-sectional area A_f . (B) Tensile force, F , leads to extension ΔL . Strain $\epsilon_f = \Delta L/L$. For an idealized linear elastic fiber, $\epsilon_f = \sigma_f/E_f$, where σ_f is the fiber tensile stress F/A_f , and E_f is the Young's modulus of the fiber. (C) Doubling fiber number halves stress and strain. (D) Shear stress, τ_f , generated at the fiber interface (yellow), equals F/A_c , where A_c is the contact area along the length of the fibers. If the cross-sectional area of the interface is small relative to A_f , $\epsilon_f \sim \Delta L/2L$. (E) Slippage caused by shear stress. Fiber extension $\Delta L'$ increases with time.

most of the cross-sectional area of the growing cell wall yet bear little tensile stress (8).

We first consider growth in one dimension. Wall growth involves two types of fiber stress: tensile and shear. If a tensile force F is applied to a fiber of length L and causes extension by



Movie 1. For a single microfibril (spring), membrane or cortical strain (elastic band) can be used to infer microfibril strain. When a weight is applied, extension of a spring (equivalent to a fiber in Fig. 1B) is the same as the extension of a less stiff elastic band attached to the spring.

¹Department of Cell and Developmental Biology, John Innes Centre, Norwich Research Park, Colney Lane, Norwich NR4 7UH, UK. ²Department of Biology, Pennsylvania State University, University Park, PA 16870, USA.

*Corresponding author. Email: enrico.coen@jic.ac.uk (E.C.); dcosgrove@psu.edu (D.J.C.)

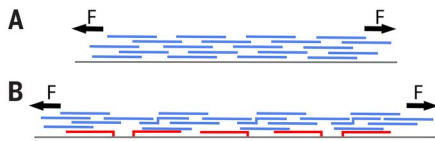


Fig. 2. Wall growth in one dimension. (A and B) Schematic of fibers in a wall cross section with the plasma membrane shown as a gray line and newly deposited fibers shown in red. Before growth is shown in (A). After growth by fiber slippage, newly deposited fibers (red) maintain wall thickness, as shown in (B).

ΔL , the proportionate increase in length, or fiber strain, is defined as $\epsilon_f = \Delta L/L$. For an idealized linear elastic fiber, fiber strain is proportional to fiber tensile stress, $\sigma_f = F/A_f$, where A_f is the fiber cross-sectional area (Fig. 1, A and B). The constant of proportionality is $1/E_f$, where E_f is Young's modulus of the fiber. If we introduce a second fiber in parallel and apply the same force, the tensile stress in each fiber is halved and fiber strain is halved (Fig. 1C), as is the strain of the entire structure or wall ϵ_w . Thus, for a given tensile force, stress and strain are inversely proportional to fiber number, N . Because of the proportionality between wall strain and fiber tensile stress, strain in cellular components that deform together with the wall, such as the plasma membrane or cortex, can be used to infer fiber stress (Movie 1).

If fibers are firmly stuck together at an interface along their length and force is applied to only one end of each fiber (Fig. 1D), a shear stress, τ_f , acts at the interface. Shear stress equals F/A_c , where A_c is the contact area along the length of the fibers. As fiber number N increases, there are more fibers and interfaces to resist the tensile force, so τ_f and σ_f decrease. As above, plasma membrane or cortical strain can be used to infer σ_f (Movie 2).

So far, we have assumed an elastic regime in which all deformations are reversible. Cell wall enlargement during growth, however, is largely irreversible, arising through slow sliding of the fiber network. Suppose τ_f exceeds a slippage threshold, such that sliding occurs at the fiber interface (yellow in Fig. 1E). In this situation, wall strain, ϵ_w , is no longer proportional to stress because wall strain continually increases in time, whereas stress does not. Thus, plasma membrane or cortical strain can no longer be used to infer fiber tensile stress (Movie 3). For a simple linear case, the rate of increase in ϵ_w , or strain rate, $\dot{\epsilon}_w$, is proportional to shear stress above the slippage threshold. The constant of proportionality, a type of “extensibility,” depends on the strength with which fibers adhere to each other (i.e., fiber-fiber binding energy). If forces are removed, individual fibers relax to their

resting lengths, but wall strain due to slippage does not reverse.

From fibers to walls

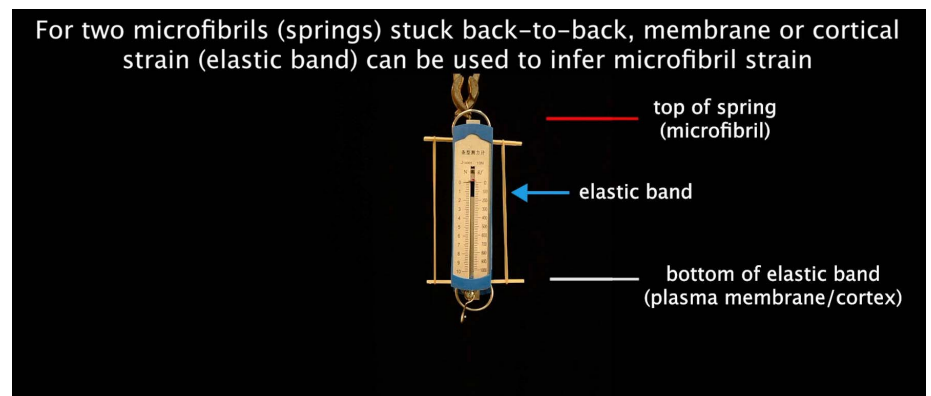
A simplified mechanical view of a growing cell wall is a network of overlapping cellulose microfibrils sticking to each other and stretched by a turgor-based tensional force F , which is maintained by cellular water uptake (Fig. 2A). Irreversible wall enlargement (~5 to 10% per hour in rapidly growing tissue) occurs at approximately constant turgor pressure through slow microfibril sliding that is facilitated by a nonenzymatic wall-loosening protein, expansin (9). As the growing wall thins through extension, wall thickness is maintained by addition of new microfibrils (red in Fig. 2B), which are synthesized at the plasma membrane, together with the incorporation of additional matrix materials. Each nascent microfibril begins to bear tensile load when it binds to overlying microfibrils that it straddles, becoming part of the cohesive cellulose network. As the overlying microfibrils slide, the nascent fiber is put under tension, “taking up the slack.”

This simplified account is consistent with the structure and nanoscale mechanics of primary cell walls (10, 11) but omits the mechanical role of matrix polysaccharides. Hemicelluloses, such as xyloglucan, bind strongly to cellulose surfaces in extended conformations and as random coils, whereas pectins form a soft hydrogel that binds weakly to cellulose surfaces (12–14). Microindentation measurements of various growing organs and pectin-rich pollen tubes have implicated pectins in the control of wall stiffness (15), whereas other experimental and computational results indicate that tensile stress is borne mainly by the cellulose network, with a minor contribution by matrix polymers (8, 16). The apparent contradiction may be partly resolved by recognizing that the in-

plane stretching of walls involves different modes of polymer deformation than out-of-plane indentation (12), with the cellulose network dominating in-plane tensile stretching and pectins contributing substantially to out-of-plane mechanics (16, 17). Pectins and xyloglucan may also influence tensile mechanics indirectly by modulating the formation of cellulose-cellulose contacts during wall assembly and remodeling, thereby shaping the cellulose network and its mechanical properties (12). Another proposal is that enzymatic swelling of pectin may supply an additional driving force for wall enlargement (14).

In addition to their structural role, pectins and xyloglucan participate in local signaling by auxin and brassinosteroid (18–20), thereby influencing many downstream pathways. Direct mechanical effects of these matrix polysaccharides may therefore be confounded with indirect hormonal responses, which complicates the interpretation of genetic studies and possibly accounts for divergent views on the effects of pectin modifications (12–14, 21–24). The role of pectins in wall mechanics and growth therefore remains contentious, and further results will be needed to reach a unified view.

In growing cell walls, lateral interfaces between aligned cellulose microfibrils are heterogeneous, involving direct cellulose-cellulose contacts, contacts mediated by a thin layer of water, and bonding through a monolayer of hemicelluloses (12, 25). The relative importance of these different interfaces for cellulose slippage has not been established. The major endogenous catalysts of cell wall extension, α -expansins, loosen noncrystalline cellulose-cellulose interactions in vitro (9), but molecular details are lacking. The loosening action of α -expansins may be restricted to infrequent sites of slippage, dubbed “biomechanical hot-spots” (12, 26). Tethering between cellulose



Movie 2. For two microfibrils (springs) stuck back to back, membrane or cortical strain (elastic band) can be used to infer microfibril strain. When a weight is applied to two firmly attached springs, extension of the springs (equivalent to fibers in Fig. 1D) is the same as the extension of a less stiff elastic band attached to the springs.

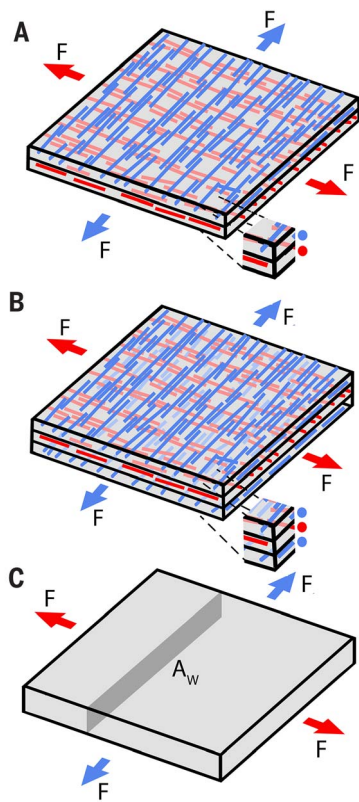


Fig. 3. Wall growth in two dimensions. (A) Two layers of microfibrils, with an equal number of microfibrils in red and blue orientations. (B) Three layers of microfibrils, with twice as many microfibrils in blue orientations than in red orientations. (C) Continuum perspective.

microfibrils by xyloglucan may also occur but contributes little to steady-state tensile mechanics (8, 26). However, mechanical responses of isolated cell walls to exogenous β 1,4-endoglucanases implicate regions of intertwined cellulose-xyloglucan in limiting cellulose sliding (16, 26).

We may also consider the wall as a continuum, rather than being made up of discrete fibers. From this perspective, wall stress, σ_w , equals F/A_w , where A_w is the wall cross-sectional area. Wall stress is less than fiber stress, because matrix contributes to the cross-sectional wall area while not bearing the main tensile load (8). Microfibril sliding, facilitated by α -expansin, can account for wall creep, which is readily observed as slow, irreversible extension of a wall held at constant force above a yield threshold (the minimum where creep begins) (9). Such sliding can dissipate wall stresses, termed wall stress relaxation, which is most apparent when wall enlargement is physically constrained (12). Stress relaxation generates the slight water potential disequilibrium required for sustained water uptake during cell enlargement (27). The stimulation of wall stress relaxation

and creep by α -expansins is maximal at acidic pH and entails changes in both the strain-rate proportionality constant, which is commonly called “wall extensibility” (2), and the yield threshold (28). This pH dependence enables rapid and local control of wall loosening by a signaling pathway that activates plasma membrane H^+ -adenosine triphosphatases (H^+ -ATPases), which acidify the wall space to activate α -expansins and promote wall creep (29). The biological control of wall pH and thereby expansin activity, which does not occur in mechanical measurements of isolated cell walls, may result in dynamic shifts in wall extensibility and the yield thresholds observed in vivo (3, 30), consistent with pH-dependent expansin action measured in vitro (28).

In addition to elasticity and creep, cell walls may also display plasticity, which is observable as an immediate irreversible deformation when tensile force is suddenly increased beyond a threshold (9, 31). Although both plasticity and creep involve cellulose-cellulose sliding, they differ in time scale and microsites of cellulose movements. Plastic deformation, unlike wall creep, is nearly independent of time and expansins and does not occur during normal cell growth, which occurs at steady turgor (steady wall stress). Sudden changes in wall tensile force (e.g., in a mechanical tester) also reveal transient mechanical responses termed viscoelastic or viscoplastic deformations. These are material responses that generally subside within a few minutes of the change in force, which reflects the short time constants of most physical rearrangements of matrix polymers and the cellulose network (other than expansin-mediated creep). Developmental patterns of wall or tissue viscoelasticity and plasticity are sometimes associated with growth (1, 15, 23), but in other cases, the correlations are poor or nonexistent (12, 32). Consequently,

the interpretation of viscoelastic-plastic measurements in relation to wall growth is a point of contention. Contrasting ideas of cell wall structure and whether tensile forces are transmitted between cellulose fibers through direct cellulose-cellulose contacts or through matrix polysaccharides lie at the heart of these divergent views (12).

Wall synthesis and loosening influence cell growth through wall creep in complementary ways (33, 34). Wall loosening increases growth rate with almost immediate effect (35), but unless wall synthesis increases in parallel, wall thickness declines over time, potentially weakening the wall. Wall synthesis requires a longer time scale to have a discernible growth effect but is critical for maintaining wall thickness and orienting anisotropy (see next section). By regulating loosening and synthesis separately, plants have the flexibility to produce rapid growth responses as well as control longer-term growth patterns and mechanical strength.

Anisotropic wall growth

Plant morphogenesis involves differential orientations and rates of growth. Such growth anisotropy is evident at the wall level, as shown by marking walls of the classically studied alga *Nitella axillaris*, whose internodes are one cell wide and grow about four times faster in length than circumference (36, 37). A key question is how growth anisotropy is determined and regulated.

Growth anisotropy depends on the three-dimensional structure of the cell wall. Consider a square piece of wall with two layers of microfibrils (colored blue and red in Fig. 3A) that are oriented perpendicular to each other. A tensile force, F , is applied to the ends of the wall equally in both microfibril orientations. If microfibrils are the main load-bearing

For two microfibrils (springs) stuck loosely together, membrane or cortical strain (elastic band) cannot be used to infer microfibril strain



Movie 3. For two microfibrils (springs) stuck loosely together, membrane or cortical strain (elastic band) cannot be used to infer microfibril strain. When a weight is applied to two springs held together with honey, slippage (as in Fig. 1E) increases with time and leads to greater strain for the elastic band than for the individual springs.

components, the average microfibril stress σ_f equals F/NA_f , where N is the number of microfibrils cut transversely in the cross section. Without microfibril slippage, wall strain, ϵ_w , equals fiber strain, ϵ_f , and is the same in both orientations. As F increases, shear stress may exceed the slippage threshold, and the wall grows at a strain rate, $\dot{\epsilon}_w$, which is the same in both orientations, giving isotropic growth.

To introduce anisotropy, we add a second layer of blue microfibrils (Fig. 3B). There are now half as many red microfibrils resisting the red force as blue resisting the blue force, so red tensile stress is twice that of blue. Red microfibrils are also under twice the shear stress of blue. As F increases, microfibrils begin to slip and exhibit faster slippage in the red direction compared with the blue direction. Thus, the orientation of maximal growth rate is aligned with the orientation of maximal microfibril stress.

Yet from a continuum perspective, wall stress, σ_w , is equal in both orientations, because A_w is the same for each (Fig. 3C). The wall Young's modulus and yield threshold (proportional to fiber slippage threshold times N) in the blue direction are twice those in the red direction. As F increases, the wall begins to yield and exhibits faster creep in the red direction compared with the blue direction. Thus, from a continuum perspective, the direction of maximal growth is coaligned with the direction of the lowest Young's modulus and wall yield threshold, whereas from a fiber perspective, maximal growth occurs in the direction of the highest microfibril stress.

From walls to cells

Modulation of wall properties can lead to formation of diverse cell geometries (38). Cell geometry may in turn feed back to influence stresses (39). In a turgid spherical cell with isotropic walls, tensile stresses are equal in all directions in the plane of the wall. However, in a cylindrical cell with isotropic walls, both wall stress and microfibril stress in the circumferential direction are twice those in the axial direction (40), which would lead to greater growth in cell diameter than length. Yet elongated cells often exhibit axial growth. Such growth may be achieved through the preferential loosening and synthesis of the wall at one end: tip growth (41). However, the cylindrical internode cells of *Nitella* grow faster axially than circumferentially even though growth is distributed throughout the wall: diffuse growth (36). Diffuse growth is common to most cells of the plant body (42).

Diffuse axial growth can be explained by wall anisotropy. Assume the wall of the cylindrical cell has twice as many circumferential microfibrils as axial microfibrils (Fig. 4). Although tensile force is twice as great in the circumferential orientation (blue arrows), there are

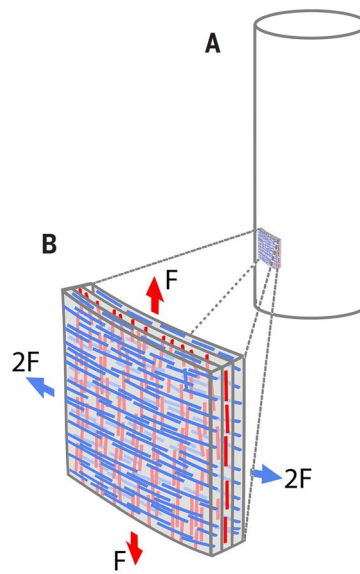


Fig. 4. Mechanics of a cylindrical cell. (A) Cell outline. (B) Microfibril composition and tensile forces on a small region of anisotropic wall with two layers of circumferential microfibrils (blue) and one layer of axial microfibrils (red).

twice as many microfibrils to resist it, and therefore microfibril stress is equal in both orientations. The wall will therefore grow equally along both the circumferential and axial directions. If the number of circumferential microfibrils is more than twice that of axial microfibrils, microfibril stress will be higher in the axial orientation and the cell grows faster in length than circumference. From a continuum perspective, resistance to wall creep is more than twice as high in the circumferential direction compared with the axial direction, leading to low circumferential growth despite twice the wall stress. Measurements on *Nitella* internode cells confirm that they have a greater proportion of circumferential to axial microfibrils and have more than twice the wall yield stress threshold in the circumferential orientation (36, 37, 43, 44).

Control of microtubule orientation in individual cells

Microfibril orientation is primarily determined by microtubules guiding cellulose synthases (45), although feedback from microfibrils can also guide cellulose synthases where microtubules are absent (46). When the growing end of a microtubule collides with another microtubule, it may turn to follow the microtubule (zippering) or undergo depolymerization (collision-induced catastrophe) (47). Computer simulations show that such interactions in a population of microtubules can generate alignments (i.e., near-parallel arrangements) that maximize microtubule survival

probability (48, 49). In a spherical cell without cues, such alignments are randomly oriented. For an elongated cell, orientations along the cell's long axis can be favored, which is consistent with longitudinal microtubule orientations that are observed in wall-less plant cells (protoplasts) deformed in rectangular microwells (50).

The predominant microtubule orientation in microwell-constrained protoplasts changes from longitudinal to transverse under high turgor, which has been explained by microtubules responding to the direction of maximal tension in the cell cortex (51). There has been confusion, however, over how stress-sensing in the cell cortex relates to sensing stresses in the wall. Stress-sensing depends on cells being able to sense strain (31), which is proportional to stress for elastic deformations (Fig. 1, A to D). Thus, for elastic deformations, cortical strain can be a proxy for measuring wall stress (Movies 1 and 2). However, in a walled cell that grows by creep, strain and wall stress are not proportional (strain can increase for a fixed stress; Fig. 1E and Movie 3). The direction of maximal strain therefore need not correspond to the direction of maximal wall stress (e.g., axially growing cylindrical cell). Thus, for an intact growing plant cell, stress-sensing in the cortex relates to wall strain, not wall stress. In principle, sudden changes in wall stress could be detected by membrane or cortical strain because creep is slow, but the relevance of such rapid stress changes to plant growth, which occurs under steady turgor, is unclear.

Various hypotheses have been proposed for how microtubules, and thus microfibrils, are oriented in intact plant cells. Classic studies on cylindrical *Nitella* cells suggested that microtubules are aligned passively by early-stage circumferential growth (52). This model was later disproved, leading to the hypothesis that microfibrils determine the directionality of cell expansion in accord with wall stress (37). One hypothesis is that membrane-spanning receptors have two domains: an extracellular domain that preferentially binds to more highly stressed microfibrils and an intracellular domain that binds to microtubules, aligning them with the direction of the bound microfibrils (53). By connecting to both microfibrils and microtubules, such receptors would allow the direction of the maximal wall stress to orient microtubules, avoiding the problem of indirect sensing through cortical or plasma membrane strain. However, enzymatic treatments, or mutants that modify mechanical properties of walls by interfering with cellulose content, have no discernible effect on microtubule patterning (54, 55), which argues against this mechanism.

Another microtubule-orienting hypothesis is based on asymmetric localization of molecules

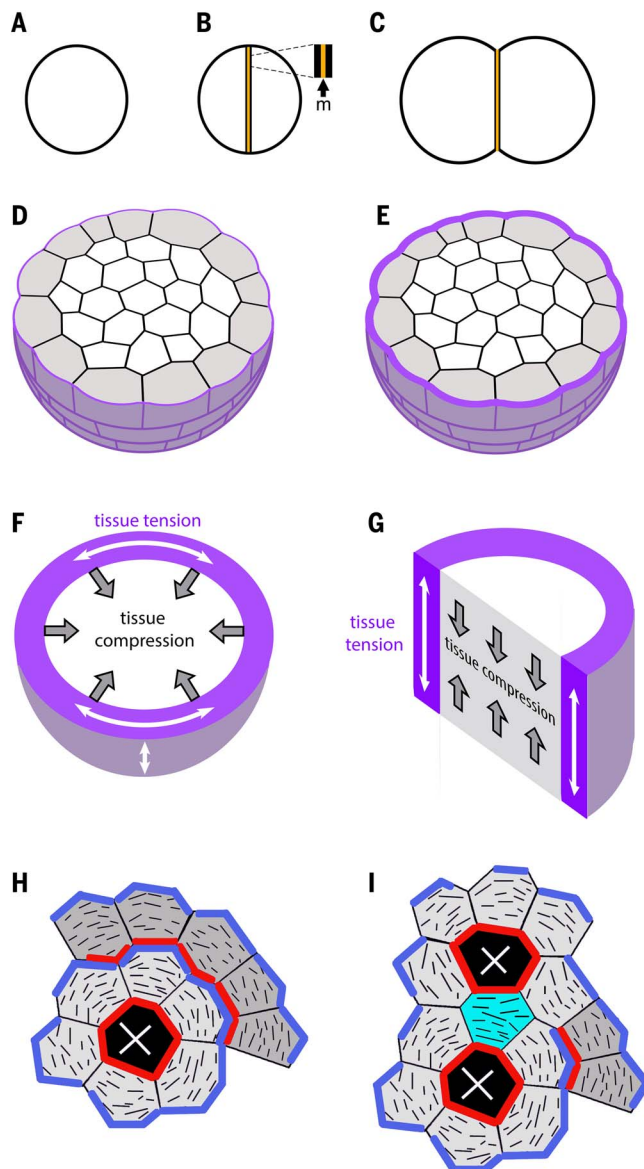


Fig. 5. Multicellular interactions. (A to C) Spherical cell (A) divides to give two daughters (B) separated by a middle lamella (yellow, m). Isotropic growth and strong adhesion lead to the formation of two cells with a flattened interface (C). (D) In a spherical tissue with isotropic walls of uniform width (shown in cross section), all walls experience similar tensile stress. The outer wall of the epidermal cells (gray) is shown in purple. (E and F) With thickened outer walls (E), growth leads to higher tensile force on the outer walls, corresponding to tissue tension in an outer region (purple) and tissue compression in the inner region of a continuous tissue (F). (G) With a cylindrical tissue that grows axially (half section shown), thickened outer walls lead to axial outer tissue tension and axial inner tissue compression. (H) With single-cell ablation (black cell with cross), microtubules (black lines) become oriented circumferentially around the wound in cells directly bordering the wound (light gray) and cells further out (dark gray). This could be explained by circumferential stresses caused by the wound orienting microtubules. Alternatively, cells could have polarity proteins (red and blue) that localize at opposite cell ends. If red polarity proteins are activated adjacent to the wound by a chemical signal, polarity proteins in cells bordering the wound would localize to faces oriented circumferentially around the wound. This polarity pattern could propagate further out (dark gray cells) through molecular signaling. Destabilization of microtubules by red and blue polarity proteins would favor microtubule orientations parallel to the red and blue faces (i.e., circumferential to the wound) because this increases microtubule survival probability. (I) In a double ablation, microtubules in the bridging cell (cyan) are oriented parallel to the cell faces adjoining the wounds, which could be explained by mechanosensing. Alternatively, red polarity proteins could be activated at both faces of the bridging cell that are adjacent to the wounds, destabilizing microtubules and favoring microtubule orientations in the bridging cell that are parallel to its two red faces.

across a cell, as exhibited by several plant polarity proteins (56–62). A cell polarity protein in protoplasts gives a polarity axis that aligns with subsequent growth orientation (63). Computer simulations show that microtubules tend to adopt orientations parallel to faces or edges where they are preferentially destabilized, because such orientations increase microtubule survival probability (48, 64). If polarity proteins at opposite end-faces or edges of a cylindrical cell destabilize microtubules, microtubule orientations parallel to the edges (i.e., circumferential) would therefore be favored. This hypothesis remains to be further explored.

Microtubule-orienting mechanisms have also been investigated for jigsaw puzzle-shaped epidermal cells (pavement cells). Microtubules on the outer face of these cells form arrays that fan out from the neck tips, which has been explained through response to stresses, localized protein activity, and/or cell geometry (65).

From cells to tissues

Morphogenesis of multicellular tissues depends not only on properties of individual cells but also on mechanical interactions between them. Consider a spherical turgid cell with isotropic walls that undergoes division (Fig. 5, A and B). With strong adhesion at the middle lamella (labeled m and colored yellow in Fig. 5B), the cells would grow to form two partial spheres joined by a flat interface (Fig. 5C). With reduced adhesion, a degree of cell separation may occur, leading to two spherical daughters in the extreme case. The extent of cell-cell adhesion is influenced by wall matrix components, such as pectins (66).

Suppose our cells continue to grow, divide, and adhere to form a spherical tissue (Fig. 5D), with an epidermal layer (gray) and all cells maintaining the same turgor. All walls have the same thickness, the same isotropic material properties, and similar tensile stress. However, if the outer epidermal walls are thicker (purple in Fig. 5E), as is common for many tissues, tensile stress is reduced in these walls because their cross-sectional area, A_w , is greater. The outer walls therefore create a growth constraint. Turgor force is then transferred from inner to outer walls, increasing the tensile force on outer walls.

Such tensile forces, or tissue tensions, have been inferred from the way tissues bend or gape after being cut or by the formation of epidermal cracks when adhesion between cells is weakened (67–69). Tissue tension can be quantified by stretching detached epidermal tissue to the point that it restores its original length (70). Epidermal tissue tension is counterbalanced by internal tissue compression—internal tissue expands when the epidermal constraint is removed. Thus, tissue stresses can be either tensile or compressive. They

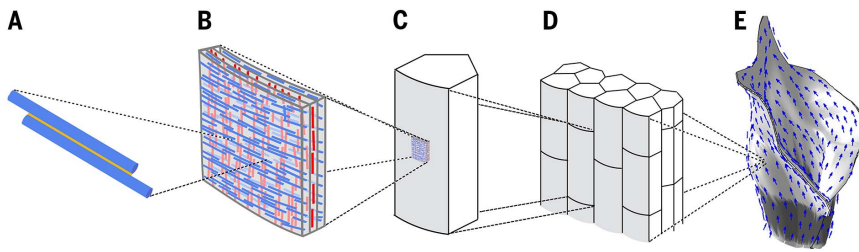


Fig. 6. Plant morphogenesis, from nano- to macroscale. (A to E) Growth begins with the sliding of cellulose fibers (A) within the cohesive, extensible, and structurally biased networks of cell walls (B). Sliding is physically driven by turgor pressure, which generates stress patterns in single cells (C) and across tissues (D). Growth may be oriented by polarity fields (blue arrows) to generate complex forms, as illustrated by a tissue-level model of grass leaf development (E), with the tubular sheath region in darker gray (93).

impose additional forces on cells that can increase or decrease wall stresses, as a result of connectivity with other cells with different mechanical or growth properties (71).

Just as wall stress is based on the notion of the wall as a continuum, tissue stress is based on the notion of tissue as a continuum (70, 72). If all regions of a continuous uniformly growing sphere have the same isotropic mechanical and growth properties, there are no tissue stresses (corresponding to all cell walls having the same thickness and wall stress). However, if the outer region of the sphere (purple in Fig. 5F) is more resistant to growth (e.g., because of thick outer cell walls), the tissue effectively behaves as a continuous pressurized vessel, with the outer region under tissue tension and the inner region under tissue compression (73) (Fig. 5F). Tissue stress does not equate to wall stress: Although tensile tissue stress is higher in the outer region, outer wall tensile stress may be reduced because of increased A_w . Similarly, although the inner region is under tissue compression, inner cell walls may partially resist some turgor force and thus be stretched in tension.

If the tissue has the form of a cylinder, thickened outer walls will lead to circumferential tissue tension being twice that of axial tissue tension. Outer wall and fiber stresses will also be greater in the circumferential orientation, resulting in axial cracks when cell adhesion is compromised, as observed with shoot apices (68).

So far, we have assumed that cell walls in our tissue have isotropic properties. Each cell would therefore grow spherically if mechanically isolated from its neighbors. If walls have anisotropic properties (e.g., biased microfibril orientations), cells in mechanical isolation would grow to form other shapes, such as ellipsoids. Oriented tissue growth may arise by coordination of such growth anisotropies between cells. For instance, if cell growth of interior cells is preferentially axial for a cylindrical tissue, thicker outer cell walls would

lead to axial outer tissue tension and axial inner tissue compression (72) (Fig. 5G), as observed in hypocotyls (67–69). Growth anisotropy of hypocotyls may be enhanced through increasing wall extensibility by brassinosteroid (32) or by selective weakening of axial walls (23).

Correlation between tissue stresses and microtubule orientations

In multicellular tissues, microtubules are typically aligned with maximal tissue tension (74, 75). For example, in shoot apical meristems, microtubules are oriented circumferentially around the apex and are aligned with organ-meristem junctions, which is the predicted orientation of maximal tissue tension (73). Wounding leads to microtubules orienting circumferentially around the wound, in alignment with predicted tissue tension (73, 76) (black lines in Fig. 5H). Mechanically bending, stretching, restraining, or compressing tissue also promotes alignments along the orientation of increased tissue tension (73, 77–80). These observations support the hypothesis that the orientation of maximal tissue tension can be sensed by cells to orient microtubules (74). Additionally, the cellulose synthesis inhibitor isoxaben alters microtubule alignments, which has been explained by wall weakening causing altered stress patterns (81, 82). However, the mechanism for sensing maximal wall-stress orientation remains speculative (74).

Another explanation may be offered for the correlation between tissue stress and microtubule orientation. Circumferential reorientation of microtubules after tissue damage may be a response that evolved to mechanically reinforce cells at the wound site, mediated by chemical signaling and cell polarity. For example, suppose cells contain two types of polarity protein, red and blue, that localize at opposite cell ends. If a wound-induced chemical signal causes the red polarity proteins to be activated in the plasma membrane adjacent to the wound site, polarity proteins in cells directly

bordering the wound would localize to cell faces oriented circumferentially around the wound (Fig. 5H). This polarity pattern could propagate further out to surrounding cells (darker gray) through cell-cell signaling (83). If red and blue polarity proteins destabilize microtubules, microtubules would become oriented circumferentially around the wound because this orientation would increase microtubule survival probability. This hypothesis is consistent with an induced pattern of cell polarity markers, which either face toward or away from the wound site (56, 82). Disruption of auxin dynamics does not prevent damage-induced cell polarity (82), indicating that polarity signaling is not auxin dependent.

Double-ablation experiments, with an intact cell between two ablated cells (cyan in Fig. 5I), were originally thought to preclude polarity as a microtubule-orienting mechanism because the cell bridging the two ablations shows circumferential microtubule orientations, even though that cell has no polarity (73). However, red polarity proteins could still be activated in the wound-facing plasma membranes of the bridging cell, destabilizing microtubules and thus orienting microtubules in the bridging cell parallel to its two red faces. Whether polarity proteins are localized in this manner for double ablations remains to be tested. Cell polarity in shoot apices may similarly provide the cue for orienting microtubules.

The effects of mechanical manipulations (bending or compressing of tissue), and of isoxaben treatment, may also have explanations that do not depend on stress sensing. Mechanical manipulations cause cells to be stretched in the direction of maximal tension, changing cell geometry. Such changes in geometry can modify microtubule orientations (50), potentially accounting for the effects of mechanical manipulations on microtubule patterns. Changes in cell geometry may be viewed as an indirect form of stress sensing in the case of mechanical manipulations. However, changes in cell geometry cannot be used as a general mechanism to infer stresses in growing plant cells. For example, in an axially growing cylindrical cell, the cell elongates axially, but wall stress is maximal circumferentially.

Isoxaben depletes cellulose synthase complexes from the plasma membrane. Because these complexes are tethered to microtubules, their depletion may affect microtubules directly rather than through the weakening of walls (54). Cellulase treatment, which weakens the wall without targeting the cellulose synthase complex, does not influence microtubule patterning (54). Similarly, mutants that reduce the amount of cellulose without impairing cellulose-synthase tethering to microtubules have little effect on microtubule patterns (55). Thus, although wall-stress sensing is often invoked to explain microtubule orientations,

the mechanosensing mechanisms remain elusive and the results may be accounted for by alternative mechanisms based on chemical signaling and cell geometry.

Stresses have also been proposed to play a role in orienting cell polarity (82). According to this view, stresses orient microtubules along the axis of maximal tension and orient cell polarity through stress gradients. However, spherical protoplasts can become polarized in the absence of mechanical asymmetries, which shows that stress gradients are not needed for polarization (63). Thus, the role of stresses versus chemical signals in the control of growth, microtubule orientation, and polarity remains controversial.

Tissue patterning and morphogenesis

Tissue morphogenesis depends on coupling the growth properties of walls, cells, and tissues to regional patterning. Coupling may occur by regional gene activity that modifies rates of microfibril deposition and/or wall extensibility and yield thresholds, and thus wall growth through creep. Regional gene activity may also provide tissue cues that orient microtubule alignments, and thus the orientations of growth anisotropy.

Computational modeling—informed by developmental genetics, live imaging, and growth analysis—has been used to determine whether such principles could account for tissue morphogenesis. From a modeling perspective, we may distinguish between two types of growth (84). “Specified growth” is how a small region of tissue would grow in isolation and therefore free from tissue stresses. “Resultant growth” is the way a small region grows when mechanically connected to the rest of the tissue. Computational models allow resultant growth, and thus tissue deformation, to be calculated from an input pattern of specified growth rates and orientations. As tissue deforms, so do the regional patterns that determine the rates and orientations of specified growth, creating a feedback loop. If cell divisions are incorporated, they are typically based on division rules and are a consequence rather than cause of growth (85–87). Such a view follows naturally from plant growth mechanics, where growth rates depend on turgor, wall extensibility, and yield thresholds instead of on the introduction of new walls, which act mechanically to restrain rather than promote growth.

Models based on regionally varying isotropic specified growth rates can account for the formation of bulges on the flanks of an apex, simulating early development of lateral appendages (primordia) (88). However, to account for more complex morphogenetic events, tissue-wide cues are needed to orient anisotropic specified growth. Use of tissue stresses to orient growth is problematic: If regions are reinforced in the direction of maximal stress,

growth will be retarded in that direction, thwarting coherent changes in tissue shape (84, 89). Tissue-stress sensing may reinforce a shape, such as leaf flatness (90), but generating a new tissue shape is more difficult. To circumvent this problem, it has been proposed that global stresses across the developing organ may be sensed (89), though how global and local stresses might be discriminated by cells remains unclear.

The stress-feedback problem does not apply when polarity controlled by chemical cues (83) is used to orient specified growth. Although tissue-wide stresses are generated through differential growth (because of tissue connectivity), they do not disrupt growth-orienting polarity fields. Moreover, tissue-wide polarity fields have been described for several polarity proteins (91). The formation of flattened structures, like leaves, can be modeled with two orthogonal polarity fields, which act in combination to orient regionally varying specified growth rates (92, 93). Leaf formation involves anisotropic growth oriented by a polarity field pointing from the tissue surface toward the ad-abaxial boundary (orthoplanar field). Orienting growth in this manner generates an initial primordial bulge followed by the development of an extended flat or curved sheet. Growth and shaping of the sheet are oriented by a second (planar) polarity field (93, 94) (Fig. 6E). Modulation of planar polarity and growth rates at the leaf margins can generate serrated forms (95). Thus, regional variation in specified growth rates, oriented by tissue-wide polarity fields, can account for a range of plant morphogenetic behaviors.

Growth arrest

Tissue growth slows down and finally arrests as plant cells mature and differentiate. Growth typically does not stop abruptly after the cessation of cell division but continues for a period, leading to cell enlargement. Growth arrest may eventually occur throughout a tissue, as with determinate organs such as leaves, or may be restricted to regions displaced away from meristems, as in stems or roots. For determinate structures, such as leaves, sepals, and the apical hook of seedlings, growth rates decline gradually with time in a defined spatial pattern (89, 94, 96–98). This decline could arise through reduced wall extensibility, an increase in yield threshold, an increase in wall thickness, and/or reduced turgor, but the contribution of each mechanism, and thus the control of final organ size, remains unclear.

Conclusion

We have reviewed the mechanics of plant morphogenesis at different interrelated levels, from fiber (Fig. 6, A and B) to wall (Fig. 6, B and C) to cell (Fig. 6, C and D) to tissue (Fig. 6, D and E). In moving up levels, a population of

discrete components is typically abstracted to a continuum at the next level (e.g., fibers to wall, walls to cell, cells to tissue). These abstractions help to both clarify concepts and simplify simulations. Mechanical stresses operate at each level, but values are typically not the same from one level to the next. By viewing the levels together, the cellulose network at the fiber and wall level provides elastic resistance to deformation while allowing growth through creep, which enables morphogenesis at the cell and tissue level while maintaining mechanical strength.

A key question is how patterns of gene expression at the tissue level modify behaviors and mechanics at other levels to generate tissue morphogenesis. Although we have outlined broad principles for how this may operate, many of the underlying molecular mechanisms are unresolved. Controversies remain over the role of pectins in controlling wall mechanics and over the role of mechanosensing or chemical signaling in controlling orientations of growth. And although tissue-level models have been proposed to account for morphogenetic changes (e.g., Fig. 6E), many of the underlying components remain hypothetical. A further challenge is to determine how interactions across levels have been modified during evolution to give rise to the diversity of plant forms (99).

To what extent can the principles of plant morphogenesis be extended to microbial and animal development? Like plants, bacteria and fungi have cell walls with fibers that confer mechanical strength but that correspond to peptidoglycans, glycans, or chitin rather than cellulose (100, 101). Growth depends on turgor, though the extent to which turgor and/or insertion of new wall material drives growth remains to be clarified (102). Animal cells have a network of fibers, the actin cortex, that lies immediately beneath the plasma membrane and plays a comparable role to a cell wall in mechanics: conferring mechanical stiffness and resistance to external mechanical stresses and turgor (103, 104). Sliding of these fibers likely plays a key role in animal morphogenesis but, unlike plants, can be active (e.g., contractile) as well as passive (caused by turgor or tissue stresses). Animal cells can rearrange and migrate during morphogenesis, but the extent of rearrangement is limited for many growing tissues, as evidenced by the coherence of clonal sectors (105–107). Thus, organogenesis presents similar issues for coordination of growth and division orientation as in plants, such as the role of polarity and stresses (108). Animal morphogenesis is also influenced mechanically and chemically by the extracellular matrix, which contains fibers, such as collagen, that may slide past each other to stretch irreversibly (109, 110). Thus, although the molecular players and interactions are different, many of

the mechanical principles and issues outlined in this review may also be applicable to microbial and animal morphogenesis.

REFERENCES AND NOTES

- A. N. J. Heyn, The physiology of cell elongation. *Bot. Rev.* **6**, 515–574 (1940). doi: [10.1007/BF02879296](https://doi.org/10.1007/BF02879296)
- J. A. Lockhart, An analysis of irreversible plant cell elongation. *J. Theor. Biol.* **8**, 264–275 (1965). doi: [10.1016/0022-5193\(65\)90077-9](https://doi.org/10.1016/0022-5193(65)90077-9); pmid: [5876240](https://pubmed.ncbi.nlm.nih.gov/5876240/)
- P. B. Green, R. O. Erickson, J. Buggy, Metabolic and physical control of cell elongation rate: In vivo studies in *Nitella*. *Plant Physiol.* **47**, 423–430 (1971). doi: [10.1104/pp.47.3.423](https://doi.org/10.1104/pp.47.3.423); pmid: [16657635](https://pubmed.ncbi.nlm.nih.gov/16657635/)
- K. T. Haas, R. Wightman, E. M. Meyerowitz, A. Peaucelle, Pectin homogalacturonan nanofilament expansion drives morphogenesis in plant epidermal cells. *Science* **367**, 1003–1007 (2020). doi: [10.1126/science.aaz5103](https://doi.org/10.1126/science.aaz5103); pmid: [32108107](https://pubmed.ncbi.nlm.nih.gov/32108107/)
- A. Ursprung, G. Blum, Eine Methode zur Messung des Wandturgordruckes der Zelle nebst Anwendungen. *Jahrb. Wiss. Bot.* **63**, 1–110 (1924).
- D. J. Cosgrove, C. T. Anderson, Plant cell growth: Do pectins drive lobe formation in arabidopsis pavement cells? *Curr. Biol.* **30**, R660–R662 (2020). doi: [10.1016/j.cub.2020.04.007](https://doi.org/10.1016/j.cub.2020.04.007); pmid: [32516619](https://pubmed.ncbi.nlm.nih.gov/32516619/)
- M. C. Jarvis, Structure of native cellulose microfibrils, the starting point for nanocellulose manufacture. *Philos. Trans. R. Soc. London Ser. A* **376**, 20170045 (2018). doi: [10.1098/rsta.2017.0045](https://doi.org/10.1098/rsta.2017.0045); pmid: [29277742](https://pubmed.ncbi.nlm.nih.gov/29277742/)
- Y. Zhang *et al.*, Molecular insights into the complex mechanics of plant epidermal cell walls. *Science* **372**, 706–711 (2021). doi: [10.1126/science.abf2824](https://doi.org/10.1126/science.abf2824); pmid: [33986175](https://pubmed.ncbi.nlm.nih.gov/33986175/)
- D. J. Cosgrove, Catalysts of plant cell wall loosening. *F1000 Res.* **5**, 119 (2016). doi: [10.12688/f1000research.7180.1](https://doi.org/10.12688/f1000research.7180.1); pmid: [26918182](https://pubmed.ncbi.nlm.nih.gov/26918182/)
- T. Zhang, D. Vavylonis, D. M. Durachko, D. J. Cosgrove, Nanoscale movements of cellulose microfibrils in primary cell walls. *Nat. Plants* **3**, 17056 (2017). doi: [10.1038/nplants.2017.56](https://doi.org/10.1038/nplants.2017.56); pmid: [28452988](https://pubmed.ncbi.nlm.nih.gov/28452988/)
- W. J. Nicolas *et al.*, Cryo-electron tomography of the onion cell wall shows bimodally oriented cellulose fibers and reticulated homogalacturonan networks. *Curr. Biol.* **32**, 2375–2389.e6 (2022). doi: [10.1016/j.cub.2022.04.024](https://doi.org/10.1016/j.cub.2022.04.024); pmid: [35508170](https://pubmed.ncbi.nlm.nih.gov/35508170/)
- D. J. Cosgrove, Building an extensible cell wall. *Plant Physiol.* **189**, 1246–1277 (2022). doi: [10.1093/plphys/kiac184](https://doi.org/10.1093/plphys/kiac184); pmid: [35460252](https://pubmed.ncbi.nlm.nih.gov/35460252/)
- A. M. Saffer, Expanding roles for pectins in plant development. *J. Integr. Plant Biol.* **60**, 910–923 (2018). doi: [10.1111/jipb.12662](https://doi.org/10.1111/jipb.12662); pmid: [29727062](https://pubmed.ncbi.nlm.nih.gov/29727062/)
- K. T. Haas, R. Wightman, A. Peaucelle, H. Höfte, The role of pectin phase separation in plant cell wall assembly and growth. *Cell Surf.* **7**, 100054 (2021). doi: [10.1016/j.ticsw.2021.100054](https://doi.org/10.1016/j.ticsw.2021.100054); pmid: [34141960](https://pubmed.ncbi.nlm.nih.gov/34141960/)
- A. J. Bidhendi, A. Geitmann, Relating the mechanics of the primary plant cell wall to morphogenesis. *J. Exp. Bot.* **67**, 449–461 (2016). doi: [10.1093/jxb/erv535](https://doi.org/10.1093/jxb/erv535); pmid: [26689854](https://pubmed.ncbi.nlm.nih.gov/26689854/)
- T. Zhang, H. Tang, D. Vavylonis, D. J. Cosgrove, Disentangling loosening from softening: Insights into primary cell wall structure. *Plant J.* **100**, 1101–1117 (2019). doi: [10.1111/tpl.14519](https://doi.org/10.1111/tpl.14519); pmid: [31469935](https://pubmed.ncbi.nlm.nih.gov/31469935/)
- M. C. Jarvis, Control of thickness of collenchyma cell walls by pectins. *Planta* **187**, 218–220 (1992). doi: [10.1007/BF00201941](https://doi.org/10.1007/BF00201941); pmid: [24178046](https://pubmed.ncbi.nlm.nih.gov/24178046/)
- J. Du, C. T. Anderson, C. Xiao, Dynamics of pectic homogalacturonan in cellular morphogenesis and adhesion, wall integrity sensing and plant development. *Nat. Plants* **8**, 332–340 (2022). doi: [10.1038/s41477-022-01120-2](https://doi.org/10.1038/s41477-022-01120-2); pmid: [35411046](https://pubmed.ncbi.nlm.nih.gov/35411046/)
- K. Jonsson, O. Hamant, R. P. Bhalerao, Plant cell walls as mechanical signaling hubs for morphogenesis. *Curr. Biol.* **32**, R334–R340 (2022). doi: [10.1016/j.cub.2022.02.036](https://doi.org/10.1016/j.cub.2022.02.036); pmid: [35413265](https://pubmed.ncbi.nlm.nih.gov/35413265/)
- Z. L. Yue *et al.*, The receptor kinase OsWAK11 monitors cell wall pectin changes to fine-tune brassinosteroid signaling and regulate cell elongation in rice. *Curr. Biol.* **32**, 2454–2466.e7 (2022). doi: [10.1016/j.cub.2022.04.028](https://doi.org/10.1016/j.cub.2022.04.028); pmid: [35521695](https://pubmed.ncbi.nlm.nih.gov/35521695/)
- G. Levesque-Tremblay, J. Pelloux, S. A. Braybrook, K. Müller, Tuning of pectin methylesterification: Consequences for cell wall biomechanics and development. *Planta* **242**, 791–811 (2015). doi: [10.1007/s00425-015-2358-5](https://doi.org/10.1007/s00425-015-2358-5); pmid: [26168980](https://pubmed.ncbi.nlm.nih.gov/26168980/)
- S. A. Braybrook, A. Peaucelle, Mechano-chemical aspects of organ formation in *Arabidopsis thaliana*: The relationship between auxin and pectin. *PLOS ONE* **8**, e57813 (2013). doi: [10.1371/journal.pone.0057813](https://doi.org/10.1371/journal.pone.0057813); pmid: [23554870](https://pubmed.ncbi.nlm.nih.gov/23554870/)
- F. Bou Daher *et al.*, Anisotropic growth is achieved through the additive mechanical effect of material anisotropy and elastic asymmetry. *eLife* **7**, e38161 (2018). doi: [10.7554/eLife.38161](https://doi.org/10.7554/eLife.38161); pmid: [30226465](https://pubmed.ncbi.nlm.nih.gov/30226465/)
- A. Peaucelle, R. Wightman, H. Höfte, The control of growth symmetry breaking in the arabidopsis hypocotyl. *Curr. Biol.* **25**, 1746–1752 (2015). doi: [10.1016/j.cub.2015.05.022](https://doi.org/10.1016/j.cub.2015.05.022); pmid: [26073136](https://pubmed.ncbi.nlm.nih.gov/26073136/)
- M. C. Jarvis, Hydrogen bonding and other non-covalent interactions at the surfaces of cellulose microfibrils. *Cellulose* **30**, 667–687 (2022). doi: [10.1007/s10570-022-04954-3](https://doi.org/10.1007/s10570-022-04954-3)
- Y. B. Park, D. J. Cosgrove, A revised architecture of primary cell walls based on biomechanical changes induced by substrate-specific endoglucanases. *Plant Physiol.* **158**, 1933–1943 (2012). doi: [10.1104/pp.111.192880](https://doi.org/10.1104/pp.111.192880); pmid: [22362871](https://pubmed.ncbi.nlm.nih.gov/22362871/)
- D. J. Cosgrove, Relaxation in a high-stress environment: The molecular bases of extensible cell walls and cell enlargement. *Plant Cell* **9**, 1031–1041 (1997). doi: [10.1105/tpc.9.7.1031](https://doi.org/10.1105/tpc.9.7.1031); pmid: [9254929](https://pubmed.ncbi.nlm.nih.gov/9254929/)
- K. Takahashi, S. Hirata, N. Kido, K. Katou, Wall-yielding properties of cell walls from elongating cucumber hypocotyls in relation to the action of expansin. *Plant Cell Physiol.* **47**, 1520–1529 (2006). doi: [10.1093/pcp/pc1017](https://doi.org/10.1093/pcp/pc1017); pmid: [17012740](https://pubmed.ncbi.nlm.nih.gov/17012740/)
- W. Lin *et al.*, TMK-based cell-surface auxin signalling activates cell-wall acidification. *Nature* **599**, 278–282 (2021). doi: [10.1038/s41586-021-03976-4](https://doi.org/10.1038/s41586-021-03976-4); pmid: [34707287](https://pubmed.ncbi.nlm.nih.gov/34707287/)
- K. Nakahori, K. Katou, H. Okamoto, Auxin changes both the extensibility and the yield threshold of the cell wall of *Vigna* hypocotyls. *Plant Cell Physiol.* **32**, 121–129 (1991).
- B. Moulia, Plant biomechanics and mechanobiology are convergent paths to flourishing interdisciplinary research. *J. Exp. Bot.* **64**, 4617–4633 (2013). doi: [10.1093/jxb/ert320](https://doi.org/10.1093/jxb/ert320); pmid: [24193603](https://pubmed.ncbi.nlm.nih.gov/24193603/)
- T. W. Wang, D. J. Cosgrove, R. N. Arteca, Brassinosteroid stimulation of hypocotyl elongation and wall relaxation in pakchoi (*Brassica chinensis* cv Lei-Choi). *Plant Physiol.* **101**, 965–968 (1993). doi: [10.1104/pp.101.3.965](https://doi.org/10.1104/pp.101.3.965); pmid: [12231748](https://pubmed.ncbi.nlm.nih.gov/12231748/)
- G. Refrégier, S. Pelletier, D. Jaillard, H. Höfte, Interaction between wall deposition and cell elongation in dark-grown hypocotyl cells in *Arabidopsis*. *Plant Physiol.* **135**, 959–968 (2004). doi: [10.1104/pp.104.038711](https://doi.org/10.1104/pp.104.038711); pmid: [15181211](https://pubmed.ncbi.nlm.nih.gov/15181211/)
- J. Verbančić, J. E. Lunn, M. Stitt, S. Persson, Carbon supply and the regulation of cell wall synthesis. *Mol. Plant* **11**, 75–94 (2018). doi: [10.1016/j.molp.2017.10.004](https://doi.org/10.1016/j.molp.2017.10.004); pmid: [29054565](https://pubmed.ncbi.nlm.nih.gov/29054565/)
- H. Edelman, R. Bergfeld, P. Schonfer, Role of cell-wall biogenesis in the initiation of auxin-mediated growth in coleoptiles of *Zea mays* L. *Planta* **179**, 486–494 (1989). doi: [10.1007/BF00397588](https://doi.org/10.1007/BF00397588); pmid: [24201772](https://pubmed.ncbi.nlm.nih.gov/24201772/)
- P. B. Green, The spiral growth pattern of the cell wall in *Nitella axillaris*. *Am. J. Bot.* **41**, 403–409 (1954). doi: [10.1002/j.1537-2197.1954.tb14356.x](https://doi.org/10.1002/j.1537-2197.1954.tb14356.x)
- P. A. Richmond, Patterns of cellulose microfibril deposition and rearrangement in *Nitella*: In vivo analysis by a birefringence index. *J. Appl. Polym. Sci.* **37**, 107–122 (1983).
- A. J. Bidhendi, A. Geitmann, Finite element modeling of shape changes in plant cells. *Plant Physiol.* **176**, 41–56 (2018). doi: [10.1104/pp.17.01684](https://doi.org/10.1104/pp.17.01684); pmid: [29229695](https://pubmed.ncbi.nlm.nih.gov/29229695/)
- A. J. Bidhendi, B. Altartouri, F. P. Gosselin, A. Geitmann, Mechanical stress initiates and sustains the morphogenesis of wavy leaf epidermal cells. *Cell Rep.* **28**, 1237–1250.e6 (2019). doi: [10.1016/j.celrep.2019.07.006](https://doi.org/10.1016/j.celrep.2019.07.006); pmid: [31365867](https://pubmed.ncbi.nlm.nih.gov/31365867/)
- E. S. Castle, Membrane tension and orientation of structure in the plant cell wall. *J. Cell. Comp. Physiol.* **10**, 113–121 (1937). doi: [10.1002/jcp.1030100110](https://doi.org/10.1002/jcp.1030100110)
- C. M. Rounds, M. Bezanilla, Growth mechanisms in tip-growing plant cells. *Annu. Rev. Plant Biol.* **64**, 243–265 (2013). doi: [10.1146/annurev-arplant-050312-120150](https://doi.org/10.1146/annurev-arplant-050312-120150); pmid: [23451782](https://pubmed.ncbi.nlm.nih.gov/23451782/)
- D. J. Cosgrove, Diffuse growth of plant cell walls. *Plant Physiol.* **176**, 16–27 (2018). doi: [10.1104/pp.17.01541](https://doi.org/10.1104/pp.17.01541); pmid: [29138349](https://pubmed.ncbi.nlm.nih.gov/29138349/)
- P. B. Green, Mechanism for plant cellular morphogenesis. *Science* **138**, 1404–1405 (1962). doi: [10.1126/science.138.3548.1404](https://doi.org/10.1126/science.138.3548.1404); pmid: [17753861](https://pubmed.ncbi.nlm.nih.gov/17753861/)
- J. P. Métraux, L. Taiz, Transverse viscoelastic extension in *Nitella*: I. Relationship to growth rate. *Plant Physiol.* **61**, 135–138 (1978). doi: [10.1104/pp.61.2.135](https://doi.org/10.1104/pp.61.2.135); pmid: [16660247](https://pubmed.ncbi.nlm.nih.gov/16660247/)
- A. R. Paredez, C. R. Somerville, D. W. Ehrhardt, Visualization of cellulose synthase demonstrates functional association with microtubules. *Science* **312**, 1491–1495 (2006). doi: [10.1126/science.1126551](https://doi.org/10.1126/science.1126551); pmid: [16627697](https://pubmed.ncbi.nlm.nih.gov/16627697/)
- J. Chan, E. Coen, Interaction between autonomous and microtubule guidance systems controls cellulose synthase trajectories. *Curr. Biol.* **30**, 941–947.e2 (2020). doi: [10.1016/j.cub.2019.12.066](https://doi.org/10.1016/j.cub.2019.12.066); pmid: [32037093](https://pubmed.ncbi.nlm.nih.gov/32037093/)
- R. Dixit, R. Cyr, Encounters between dynamic cortical microtubules promote ordering of the cortical array through angle-dependent modifications of microtubule behavior. *Plant Cell* **16**, 3274–3284 (2004). doi: [10.1105/tpc.104.026930](https://doi.org/10.1105/tpc.104.026930); pmid: [15539470](https://pubmed.ncbi.nlm.nih.gov/15539470/)
- B. Chakraborty, I. Biliou, B. Scheres, B. M. Mulder, A computational framework for cortical microtubule dynamics in realistically shaped plant cells. *PLOS Comput. Biol.* **14**, e1005959 (2018). doi: [10.1371/journal.pcbi.1005959](https://doi.org/10.1371/journal.pcbi.1005959); pmid: [29394250](https://pubmed.ncbi.nlm.nih.gov/29394250/)
- S. H. Tindemans, R. J. Hawkins, B. M. Mulder, Survival of the aligned: Ordering of the plant cortical microtubule array. *Phys. Rev. Lett.* **104**, 058103 (2010). doi: [10.1103/PhysRevLett.104.058103](https://doi.org/10.1103/PhysRevLett.104.058103); pmid: [20366797](https://pubmed.ncbi.nlm.nih.gov/20366797/)
- P. Durand-Smet, T. A. Spelman, E. M. Meyerowitz, H. Jönsson, Cytoskeletal organization in isolated plant cells under geometry control. *Proc. Natl. Acad. Sci. U.S.A.* **117**, 17399–17408 (2020). doi: [10.1073/pnas.2003184117](https://doi.org/10.1073/pnas.2003184117); pmid: [32641513](https://pubmed.ncbi.nlm.nih.gov/32641513/)
- L. Colin *et al.*, Cortical tension overrides geometrical cues to orient microtubules in confined protoplasts. *Proc. Natl. Acad. Sci. U.S.A.* **117**, 32731–32738 (2020). doi: [10.1073/pnas.2008895117](https://doi.org/10.1073/pnas.2008895117); pmid: [33288703](https://pubmed.ncbi.nlm.nih.gov/33288703/)
- P. B. Green, A. King, A mechanism for the origin of specifically oriented textures in development with special reference to *Nitella* wall texture. *Aust. J. Biol. Sci.* **19**, 421–437 (1966). doi: [10.1071/BI9660421](https://doi.org/10.1071/BI9660421)
- R. E. Williamson, Alignment of cortical microtubules by anisotropic wall stresses. *Aust. J. Plant Physiol.* **17**, 601–613 (1990).
- A. R. Paredez, S. Persson, D. W. Ehrhardt, C. R. Somerville, Genetic evidence that cellulose synthase activity influences microtubule cortical array organization. *Plant Physiol.* **147**, 1723–1734 (2008). doi: [10.1104/pp.108.120196](https://doi.org/10.1104/pp.108.120196); pmid: [18583534](https://pubmed.ncbi.nlm.nih.gov/18583534/)
- R. Schneider, D. W. Ehrhardt, E. M. Meyerowitz, A. Sampathkumar, Tethering of cellulose synthase to microtubules dampens mechano-induced cytoskeletal organization in *Arabidopsis* pavement cells. *Nat. Plants* **8**, 1064–1073 (2022). doi: [10.1038/s41477-022-01218-7](https://doi.org/10.1038/s41477-022-01218-7); pmid: [35982303](https://pubmed.ncbi.nlm.nih.gov/35982303/)
- M. Bringmann, D. C. Bergmann, Tissue-wide mechanical forces influence the polarity of stomatal stem cells in *Arabidopsis*. *Curr. Biol.* **27**, 877–883 (2017). doi: [10.1016/j.cub.2017.01.059](https://doi.org/10.1016/j.cub.2017.01.059); pmid: [28285992](https://pubmed.ncbi.nlm.nih.gov/28285992/)
- P. Křeček *et al.*, The PIN-FORMED (PIN) protein family of auxin transporters. *Genome Biol.* **10**, 249 (2009). doi: [10.1186/gb-2009-10-12-249](https://doi.org/10.1186/gb-2009-10-12-249); pmid: [20053306](https://pubmed.ncbi.nlm.nih.gov/20053306/)
- J. Dong, C. A. MacAlister, D. C. Bergmann, BASL controls asymmetric cell division in *Arabidopsis*. *Cell* **137**, 1320–1330 (2009). doi: [10.1016/j.cell.2009.04.018](https://doi.org/10.1016/j.cell.2009.04.018); pmid: [19523675](https://pubmed.ncbi.nlm.nih.gov/19523675/)
- E. Truernit *et al.*, High-resolution whole-mount imaging of three-dimensional tissue organization and gene expression enables the study of phloem development and structure in *Arabidopsis*. *Plant Cell* **20**, 1494–1503 (2008). doi: [10.1105/tpc.107.056069](https://doi.org/10.1105/tpc.107.056069); pmid: [18523061](https://pubmed.ncbi.nlm.nih.gov/18523061/)
- S. Yoshida *et al.*, A SOSEKI-based coordinate system interprets global polarity cues in *Arabidopsis*. *Nat. Plants* **5**, 160–166 (2019). doi: [10.1038/s41477-019-0363-6](https://doi.org/10.1038/s41477-019-0363-6); pmid: [30737509](https://pubmed.ncbi.nlm.nih.gov/30737509/)
- L. J. Pilitter, K. M. Peterson, R. J. Horst, K. U. Torii, Molecular profiling of stomatal meristemoids reveals new component of asymmetric cell division and commonalities among stem cell populations in *Arabidopsis*. *Plant Cell* **23**, 3260–3275 (2011). doi: [10.1105/tpc.111.088583](https://doi.org/10.1105/tpc.111.088583); pmid: [21963668](https://pubmed.ncbi.nlm.nih.gov/21963668/)
- E. Truernit, H. Bauby, K. Belcram, J. Barthélémy, J. C. Palauqui, OCTOPUS, a polarly localised membrane-associated protein, regulates phloem differentiation entry in *Arabidopsis thaliana*. *Development* **139**, 1306–1315 (2012). doi: [10.1242/dev.072629](https://doi.org/10.1242/dev.072629); pmid: [22395740](https://pubmed.ncbi.nlm.nih.gov/22395740/)
- J. Chan, C. Mansfield, F. Clouet, D. Dorussen, E. Coen, Intrinsic cell polarity coupled to growth axis formation in tobacco BY-2 cells. *Curr. Biol.* **30**, 4999–5006.e3 (2020). doi: [10.1016/j.cub.2020.09.036](https://doi.org/10.1016/j.cub.2020.09.036); pmid: [33035485](https://pubmed.ncbi.nlm.nih.gov/33035485/)

64. C. Ambrose, J. F. Allard, E. N. Cytrynbaum, G. O. Wasteneys, A CLASP-modulated cell edge barrier mechanism drives cell-wide cortical microtubule organization in *Arabidopsis*. *Nat. Commun.* **2**, 430 (2011). doi: [10.1038/ncomms1444](https://doi.org/10.1038/ncomms1444); pmid: [21847104](https://pubmed.ncbi.nlm.nih.gov/21847104/)
65. S. Liu, F. Jobert, Z. Rahnesan, S. M. Doyle, S. Robert, Solving the puzzle of shape regulation in plant epidermal pavement cells. *Annu. Rev. Plant Biol.* **72**, 525–550 (2021). doi: [10.1146/annurev-arplant-080720-081920](https://doi.org/10.1146/annurev-arplant-080720-081920); pmid: [34143651](https://pubmed.ncbi.nlm.nih.gov/34143651/)
66. F. B. Daher, S. A. Braybrook, How to let go: Pectin and plant cell adhesion. *Front. Plant Sci.* **6**, 523 (2015). doi: [10.3389/fpls.2015.00523](https://doi.org/10.3389/fpls.2015.00523); pmid: [26236321](https://pubmed.ncbi.nlm.nih.gov/26236321/)
67. W. S. Peters, A. D. Tomos, The history of tissue tension. *Ann. Bot.* **77**, 657–665 (1996). doi: [10.1093/aob/77.6.657](https://doi.org/10.1093/aob/77.6.657); pmid: [11541099](https://pubmed.ncbi.nlm.nih.gov/11541099/)
68. S. Verger, Y. Long, A. Boudaoud, O. Hamant, A tension-adhesion feedback loop in plant epidermis. *eLife* **7**, e34460 (2018). doi: [10.7554/eLife.34460](https://doi.org/10.7554/eLife.34460); pmid: [29683428](https://pubmed.ncbi.nlm.nih.gov/29683428/)
69. U. Kutschera, K. J. Niklas, The epidermal-growth-control theory of stem elongation: An old and a new perspective. *J. Plant Physiol.* **164**, 1395–1409 (2007). doi: [10.1016/j.jplph.2007.08.002](https://doi.org/10.1016/j.jplph.2007.08.002); pmid: [17905474](https://pubmed.ncbi.nlm.nih.gov/17905474/)
70. Z. Hejnowicz, A. Sievers, Tissue stresses in organs of herbaceous plants II. Determination in three dimensions in the hypocotyl of sunflower. *J. Exp. Bot.* **46**, 1045–1053 (1995). doi: [10.1093/jxb/46.8.1045](https://doi.org/10.1093/jxb/46.8.1045)
71. Z. Hejnowicz, A. Sievers, Tissue stresses in organs of herbaceous plants I. Poisson ratios of tissues and their role in determination of the stresses. *J. Exp. Bot.* **289**, 1035–1043 (1995). doi: [10.1093/jxb/46.8.1035](https://doi.org/10.1093/jxb/46.8.1035)
72. A. Goriely, *The Mathematics and Mechanics of Biological Growth* (Springer, 2017).
73. O. Hamant *et al.*, Developmental patterning by mechanical signals in *Arabidopsis*. *Science* **322**, 1650–1655 (2008). doi: [10.1126/science.1165594](https://doi.org/10.1126/science.1165594); pmid: [19074340](https://pubmed.ncbi.nlm.nih.gov/19074340/)
74. O. Hamant, D. Inoue, D. Bouchez, J. Dumais, E. Mjølness, Are microtubules tension sensors? *Nat. Commun.* **10**, 2360 (2019). doi: [10.1038/s41467-019-10207-y](https://doi.org/10.1038/s41467-019-10207-y); pmid: [31142740](https://pubmed.ncbi.nlm.nih.gov/31142740/)
75. M. G. Heisler, Integration of core mechanisms underlying plant aerial architecture. *Front. Plant Sci.* **12**, 786338 (2021). doi: [10.3389/fpls.2021.786338](https://doi.org/10.3389/fpls.2021.786338); pmid: [34868186](https://pubmed.ncbi.nlm.nih.gov/34868186/)
76. J. M. Hush, C. R. Hawes, R. L. Overall, Interphase microtubule re-orientation predicts a new cell polarity in wounded pea roots. *J. Cell Sci.* **96**, 47–61 (1990). doi: [10.1242/jcs.96.1.47](https://doi.org/10.1242/jcs.96.1.47)
77. Z. Hejnowicz, A. Rusin, T. Rusin, Tensile tissue stress affects the orientation of cortical microtubules in the epidermis of sunflower hypocotyl. *J. Plant Growth Regul.* **19**, 31–44 (2000). doi: [10.1007/s003440000005](https://doi.org/10.1007/s003440000005); pmid: [11010990](https://pubmed.ncbi.nlm.nih.gov/11010990/)
78. A. Burian, Z. Hejnowicz, Strain rate does not affect cortical microtubule orientation in the isolated epidermis of sunflower hypocotyls. *Plant Biol.* **12**, 459–468 (2010). doi: [10.1111/j.1438-8677.2009.00228.x](https://doi.org/10.1111/j.1438-8677.2009.00228.x); pmid: [20522182](https://pubmed.ncbi.nlm.nih.gov/20522182/)
79. S. Robinson, C. Kuhlemeier, Global compression reorients cortical microtubules in *Arabidopsis* hypocotyl epidermis and promotes growth. *Curr. Biol.* **28**, 1794–1802.e2 (2018). doi: [10.1016/j.cub.2018.04.028](https://doi.org/10.1016/j.cub.2018.04.028); pmid: [29804811](https://pubmed.ncbi.nlm.nih.gov/29804811/)
80. K. Zandomeni, P. Schopfer, Mechanosensory microtubule reorientation in the epidermis of maize coleoptiles subjected to bending stress. *Protoplasma* **182**, 96–101 (1994). doi: [10.1007/BF01403471](https://doi.org/10.1007/BF01403471); pmid: [11540618](https://pubmed.ncbi.nlm.nih.gov/11540618/)
81. D. D. Fisher, R. J. Cyr, Extending the microtubule/microfibril paradigm: Cellulose synthesis is required for normal cortical microtubule alignment in elongating cells. *Plant Physiol.* **116**, 1043–1051 (1998). doi: [10.1104/pp.116.3.1043](https://doi.org/10.1104/pp.116.3.1043); pmid: [9501137](https://pubmed.ncbi.nlm.nih.gov/9501137/)
82. M. G. Heisler *et al.*, Alignment between PIN1 polarity and microtubule orientation in the shoot apical meristem reveals a tight coupling between morphogenesis and auxin transport. *PLoS Biol.* **8**, e1000516 (2010). doi: [10.1371/journal.pbio.1000516](https://doi.org/10.1371/journal.pbio.1000516); pmid: [20976043](https://pubmed.ncbi.nlm.nih.gov/20976043/)
83. K. Abley *et al.*, An intracellular partitioning-based framework for tissue cell polarity in plants and animals. *Development* **140**, 2061–2074 (2013). doi: [10.1242/dev.062984](https://doi.org/10.1242/dev.062984); pmid: [23633507](https://pubmed.ncbi.nlm.nih.gov/23633507/)
84. E. Coen, R. Kennaway, C. Whitewoods, On genes and form. *Development* **144**, 4203–4213 (2017). doi: [10.1242/dev.151910](https://doi.org/10.1242/dev.151910); pmid: [29183934](https://pubmed.ncbi.nlm.nih.gov/29183934/)
85. L. Errera, Sur une condition fondamentale d'équilibre des cellules vivantes. *C.R. Acad. Sci.* **103**, 822–824 (1886).
86. P. Prusinkiewicz, A. Runions, Computational models of plant development and form. *New Phytol.* **193**, 549–569 (2012). doi: [10.1111/j.1469-8137.2011.04009.x](https://doi.org/10.1111/j.1469-8137.2011.04009.x); pmid: [22235985](https://pubmed.ncbi.nlm.nih.gov/22235985/)
87. S. Yoshida *et al.*, Genetic control of plant development by overriding a geometric division rule. *Dev. Cell* **29**, 75–87 (2014). doi: [10.1016/j.devcel.2014.02.002](https://doi.org/10.1016/j.devcel.2014.02.002); pmid: [24684831](https://pubmed.ncbi.nlm.nih.gov/24684831/)
88. F. Boudon *et al.*, A computational framework for 3D mechanical modeling of plant morphogenesis with cellular resolution. *PLoS Comput. Biol.* **11**, e1003950 (2015). doi: [10.1371/journal.pcbi.1003950](https://doi.org/10.1371/journal.pcbi.1003950); pmid: [25569615](https://pubmed.ncbi.nlm.nih.gov/25569615/)
89. N. Hervieux *et al.*, A mechanical feedback restricts sepal growth and shape in *Arabidopsis*. *Curr. Biol.* **26**, 1019–1028 (2016). doi: [10.1016/j.cub.2016.03.004](https://doi.org/10.1016/j.cub.2016.03.004); pmid: [27151660](https://pubmed.ncbi.nlm.nih.gov/27151660/)
90. F. Zhao *et al.*, Microtubule-mediated wall anisotropy contributes to leaf blade flattening. *Curr. Biol.* **30**, 3972–3985.e6 (2020). doi: [10.1016/j.cub.2020.07.076](https://doi.org/10.1016/j.cub.2020.07.076); pmid: [32916107](https://pubmed.ncbi.nlm.nih.gov/32916107/)
91. V. Gorelova, J. Sprakel, D. Weijers, Plant cell polarity as the nexus of tissue mechanics and morphogenesis. *Nat. Plants* **7**, 1548–1559 (2021). doi: [10.1038/s41477-021-01021-w](https://doi.org/10.1038/s41477-021-01021-w); pmid: [34887521](https://pubmed.ncbi.nlm.nih.gov/34887521/)
92. C. D. Whitewoods *et al.*, Evolution of carnivorous traps from planar leaves through simple shifts in gene expression. *Science* **367**, 91–96 (2020). doi: [10.1126/science.aay5433](https://doi.org/10.1126/science.aay5433); pmid: [31753850](https://pubmed.ncbi.nlm.nih.gov/31753850/)
93. A. E. Richardson *et al.*, Evolution of the grass leaf by primordium extension and petiole-lamina remodeling. *Science* **374**, 1377–1381 (2021). doi: [10.1126/science.abc9407](https://doi.org/10.1126/science.abc9407); pmid: [34882477](https://pubmed.ncbi.nlm.nih.gov/34882477/)
94. S. Fox *et al.*, Spatiotemporal coordination of cell division and growth during organ morphogenesis. *PLoS Biol.* **16**, e2005952 (2018). doi: [10.1371/journal.pbio.2005952](https://doi.org/10.1371/journal.pbio.2005952); pmid: [30383040](https://pubmed.ncbi.nlm.nih.gov/30383040/)
95. D. Kierzkowski *et al.*, A growth-based framework for leaf shape development and diversity. *Cell* **177**, 1405–1418.e17 (2019). doi: [10.1016/j.cell.2019.05.011](https://doi.org/10.1016/j.cell.2019.05.011); pmid: [31130379](https://pubmed.ncbi.nlm.nih.gov/31130379/)
96. M. Zhu *et al.*, Robust organ size requires robust timing of initiation orchestrated by focused auxin and cytokinin signalling. *Nat. Plants* **6**, 686–698 (2020). doi: [10.1038/s41477-020-0666-7](https://doi.org/10.1038/s41477-020-0666-7); pmid: [32451448](https://pubmed.ncbi.nlm.nih.gov/32451448/)
97. P. Žádníková *et al.*, a model of differential growth-guided apical hook formation in plants. *Plant Cell* **28**, 2464–2477 (2016). doi: [10.1105/tpc.15.00569](https://doi.org/10.1105/tpc.15.00569); pmid: [27754878](https://pubmed.ncbi.nlm.nih.gov/27754878/)
98. Q. Zhu, P. Žádníková, D. Smet, D. Van Der Straeten, E. Benková, Real-time analysis of the apical hook development. *Methods Mol. Biol.* **1497**, 1–8 (2017). doi: [10.1007/978-1-4939-6469-7_1](https://doi.org/10.1007/978-1-4939-6469-7_1); pmid: [27864752](https://pubmed.ncbi.nlm.nih.gov/27864752/)
99. D. Wilson-Sánchez, N. Bhatia, A. Runions, M. Tsiantis, From genes to shape in leaf development and evolution. *Curr. Biol.* **32**, R1215–R1222 (2022). doi: [10.1016/j.cub.2022.09.021](https://doi.org/10.1016/j.cub.2022.09.021); pmid: [36347226](https://pubmed.ncbi.nlm.nih.gov/36347226/)
100. N. A. R. Gow, M. D. Lenardon, Architecture of the dynamic fungal cell wall. *Nat. Rev. Microbiol.* **10.1038/s41579-022-00796-9** (2022). doi: [10.1038/s41579-022-00796-9](https://doi.org/10.1038/s41579-022-00796-9); pmid: [36266346](https://pubmed.ncbi.nlm.nih.gov/36266346/)
101. T. Dörr, P. J. Moynihan, C. Mayer, Editorial: Bacterial cell wall structure and dynamics. *Front. Microbiol.* **10**, 2051 (2019). doi: [10.3389/fmicb.2019.02051](https://doi.org/10.3389/fmicb.2019.02051); pmid: [31551985](https://pubmed.ncbi.nlm.nih.gov/31551985/)
102. E. R. Rojas, K. C. Huang, Regulation of microbial growth by turgor pressure. *Curr. Opin. Microbiol.* **42**, 62–70 (2018). doi: [10.1016/j.mib.2017.10.015](https://doi.org/10.1016/j.mib.2017.10.015); pmid: [29125939](https://pubmed.ncbi.nlm.nih.gov/29125939/)
103. G. Salbreux, G. Charras, E. Paluch, Actin cortex mechanics and cellular morphogenesis. *Trends Cell Biol.* **22**, 536–545 (2012). doi: [10.1016/j.tcb.2012.07.001](https://doi.org/10.1016/j.tcb.2012.07.001); pmid: [22871642](https://pubmed.ncbi.nlm.nih.gov/22871642/)
104. T. Kim, M. L. Gardel, E. Munro, Determinants of fluidlike behavior and effective viscosity in cross-linked actin networks. *Biophys. J.* **106**, 526–534 (2014). doi: [10.1016/j.bpj.2013.12.031](https://doi.org/10.1016/j.bpj.2013.12.031); pmid: [24507593](https://pubmed.ncbi.nlm.nih.gov/24507593/)
105. L. Marcon, C. G. Arqués, M. S. Torres, J. Sharpe, A computational clonal analysis of the developing mouse limb bud. *PLoS Comput. Biol.* **7**, e1001071 (2011). doi: [10.1371/journal.pcbi.1001071](https://doi.org/10.1371/journal.pcbi.1001071); pmid: [21347315](https://pubmed.ncbi.nlm.nih.gov/21347315/)
106. S. M. Meilhac *et al.*, A retrospective clonal analysis of the myocardium reveals two phases of clonal growth in the developing mouse heart. *Development* **130**, 3877–3889 (2003). doi: [10.1242/dev.00580](https://doi.org/10.1242/dev.00580); pmid: [12835402](https://pubmed.ncbi.nlm.nih.gov/12835402/)
107. F. Germani, C. Bergantinos, L. A. Johnston, Mosaic analysis in *Drosophila*. *Genetics* **208**, 473–490 (2018). doi: [10.1534/genetics.117.300256](https://doi.org/10.1534/genetics.117.300256); pmid: [29378809](https://pubmed.ncbi.nlm.nih.gov/29378809/)
108. L. LeGoff, T. Lecuit, Mechanical forces and growth in animal tissues. *Cold Spring Harb. Perspect. Biol.* **8**, a019232 (2015). doi: [10.1101/cshperspect.a019232](https://doi.org/10.1101/cshperspect.a019232); pmid: [26261279](https://pubmed.ncbi.nlm.nih.gov/26261279/)
109. B. Sun, The mechanics of fibrillar collagen extracellular matrix. *Cell Rep. Phys. Sci.* **2**, 100515 (2021). doi: [10.1016/j.xcrp.2021.100515](https://doi.org/10.1016/j.xcrp.2021.100515); pmid: [34485951](https://pubmed.ncbi.nlm.nih.gov/34485951/)
110. M. L. Wood, G. E. Lester, L. E. Dahners, Collagen fiber sliding during ligament growth and contracture. *J. Orthop. Res.* **16**, 438–440 (1998). doi: [10.1002/jor.1100160407](https://doi.org/10.1002/jor.1100160407); pmid: [9747784](https://pubmed.ncbi.nlm.nih.gov/9747784/)

ACKNOWLEDGMENTS

We thank P. Robinson for filming and editing the movies and J. Chan, P. Durand-Smet, A. Hanner, R. Kennaway, R. Smith, and S. Zhang for helpful comments on the manuscript. **Funding:** We acknowledge support from the Human Frontier Science Program (HFSP) for a collaborative research grant RGP0005/2022 awarded to the authors of this review. E.C. was supported by grants from the UK Biotechnology and Biological Sciences Research Council (BB/M023117/1, BB/W007924/1, BBS/E/J/000PR9787, BBS/E/J/00000152, BB/L008920/1, and BBS/E/J/000PR9789). D.J.C. was supported by the US Department of Energy under awards #DE-SC0001090 for work on wall structure and #DE-FG2-84ER13179 for work on expansins and wall mechanics. **Competing interests:** The authors have no competing interests. **License information:** Copyright © 2023 the authors, some rights reserved; exclusive licensee American Association for the Advancement of Science. No claim to original US government works. <https://www.science.org/about/science-licenses-journal-article-reuse>

Submitted 3 October 2022; accepted 15 December 2022
10.1126/science.ade8055